Mol Neurobiol (2012) 45:440–454
DOI 10.1007/s12035-012-8256-y

TUDCA, a Bile Acid, Attenuates Amyloid Precursor Protein Processing and Amyloid-β Deposition in APP/PS1 Mice

Ana F. Nunes · Joana D. Amaral · Adrian C. Lo · Maria B. Fonseca · Ricardo J. S. Viana · Zsuzsanna Callaerts-Vegh · Rudi D'Hooge · Cecília M. P. Rodrigues

Received: 21 December 2011 / Accepted: 1 March 2012 / Published online: 23 March 2012

Abstract Alzheimer's disease (AD) is a neurodegenerative disorder characterized by accumulation of amyloid-β (Aβ) peptide in the hippocampus and frontal cortex of the brain, leading to progressive cognitive decline. The endogenous bile acid tauroursodeoxycholic acid (TUDCA) is a strong neuroprotective agent in several experimental models of disease, including neuronal exposure to Aβ. Nevertheless, the therapeutic role of TUDCA in AD pathology has not yet been ascertained. Here we report that feeding APP/PS1 double-transgenic mice with diet containing 0.4 % TUDCA for 6 months reduced accumulation of Aβ deposits in the brain, markedly ameliorating memory deficits. This was accompanied by reduced glial activation and neuronal integrity loss in TUDCA-fed APP/PS1 mice compared to untreated APP/PS1 mice. Furthermore, TUDCA regulated lipid-metabolism mediators involved in Aβ production and accumulation in the brains of transgenic mice. Overall amyloidogenic APP processing was reduced with TUDCA treatment, in association with, but not limited to, modulation of γ-secretase activity. Consequently, a significant decrease in $Aβ_{1–40}$ and $Aβ_{1–42}$ levels was observed in both hippocampus and frontal cortex of TUDCA-treated APP/PS1 mice, suggesting that chronic feeding of TUDCA interferes with Aβ production, possibly through the regulation of lipid-metabolism mediators associated with APP processing. These results highlight TUDCA as a potential therapeutic strategy for the prevention and treatment of AD.

Keywords Aβ load · Alzheimer's disease · Lipid metabolism · γ-Secretase · TUDCA

A. F. Nunes · J. D. Amaral · M. B. Fonseca · R. J. S. Viana · C. M. P. Rodrigues (✉)
Research Institute for Medicines and Pharmaceutical Sciences (iMed.UL), Faculty of Pharmacy, University of Lisbon, Lisbon 1649-003, Portugal
e-mail: cmprodrigues@ff.ul.pt

A. C. Lo · Z. Callaerts-Vegh · R. D'Hooge
Laboratory of Biological Psychology, University of Leuven, Leuven, Belgium

C. M. P. Rodrigues
Department of Biochemistry and Human Biology, Faculty of Pharmacy, University of Lisbon, Lisbon, Portugal

Introduction

Alzheimer's disease (AD) is the most prevalent form of dementia, resulting in progressive neuronal death and debilitating damage to brain loci that mediate memory and higher cognitive function [1]. Accumulation of amyloid-β (Aβ) peptide has been shown to play a critical role in the pathogenesis of AD. Among its two predominant forms, $Aβ_{1–42}$ possesses stronger aggregation and deposition propensity than $Aβ_{1–40}$ [1]. Accumulation of Aβ in the brain is associated with mutations in amyloid precursor protein (*APP*) [2], presenilin 1 (*PS1*) [3], and presenilin 2 (*PS2*) [4] genes. Aβ peptides are generated by successive proteolysis of APP, a large transmembrane glycoprotein that is initially cleaved by β-secretase, and subsequently by γ-secretase in the transmembrane domain [5–7]. The γ-secretase complex consists of presenilin and at least three other integral membrane proteins [8]. Usually, γ-secretase does not proteolyze the full-length proteins, but so-called COOH-terminal fragments (CTFs), produced from the full-length proteins by another protease. While pathogenic mutations have been implicated in ~2 % of AD cases, the proximal events that underlie the common, sporadic form of the disease are incompletely understood.

The major genetic risk factor for late-onset AD is the presence of the ε4 allele of the apolipoprotein E (*APOE*) gene [9], which encodes a protein that contributes to AD pathogenesis by modulating the metabolism and aggregation of Aβ peptide and by directly regulating brain lipid metabolism and synaptic function through APOE receptors (reviewed in [10]). Based on genetic evidence, α_2−macroglubulin (*A2M*) gene is recognized as the second confirmed late-onset AD gene (reviewed in [11]). DNA polymorphisms in the *A2M* gene associated with AD result in significantly increased deposition of Aβ in AD brains. This APOE receptor ligand, like APOE itself, binds Aβ with high specificity and is present in AD senile plaques [11]. Another APOE-binding protein is sortilin-related receptor with A-type repeats (SORLA; also known as SORL1 and LR11). Recent work suggests that SORLA may play a protective role in AD by reducing APP processing and generation of Aβ peptides [12]. Curiously, this lipoprotein receptor is also genetically associated with late-onset AD [13].

Over the past decades, the molecules that control APP processing into Aβ have been the focus of intense investigation. In this respect, connective tissue growth factor (CTGF) has been recently implicated in AD pathogenesis by increasing Aβ peptides steady-state levels, possibly through a mechanism that involves γ-secretase activation [14]. Much like APOE, A2M and SORLA, CTGF is a ligand for the low-density lipoprotein receptor-related protein [15–17], and its expression correlates with the progression of AD clinical dementia and amyloid neuritic plaque neuropathology [14].

We have previously shown that the endogenous bile acid tauroursodeoxycholic acid (TUDCA) is a potent anti-apoptotic agent in neuronal cells exposed to Aβ and a powerful neuroprotective strategy in animal models of neuronal degeneration [18–21]. TUDCA specifically modulates Aβ-induced toxicity by inhibiting organelle-driven apoptosis [22] and interfering with upstream molecular targets of p53 pathways [23–25], although without changing secondary structures and fibrillogenic propensities of Aβ peptides in vitro [26]. The molecular mechanisms underlying TUDCA neuroprotective properties appear to be complex and may engage a number of different molecular targets, possibly involving gene regulation. The marked downregulation of A2M and CTGF expression by TUDCA [27] suggests that TUDCA could be a potential therapeutic strategy in AD. TUDCA is strongly neuroprotective in pharmacologic and transgenic animal models of Huntington's disease [18, 19], in ischemic and hemorrhagic stroke [20, 21], and in cellular models of AD [22–25]. TUDCA is an orally bioavailable and central nervous system penetrating agent, known to cross blood–brain barrier [18]. A recent clinical study showed that unconjugated UDCA is safe and well tolerated in amyotrophic lateral sclerosis, documenting effective and dose-dependent cerebrospinal fluid penetration [28]. Given the effect of TUDCA in regulating lipid metabolism gene expression and the role of lipid mediators in modulating Aβ metabolism, we hypothesize that TUDCA reduces Aβ toxicity by interfering with its production and accumulation. This hypothesis was investigated in APP/PS1 mice, a well-established AD mouse model of Aβ aggregation [29].

Materials and Methods

Transgenic Mice and TUDCA Treatment APP/PS1 double-transgenic mice express human APP containing the KM670/671NL Swedish double mutation and human PS1 carrying the L166P mutation under the control of a neuron-specific murine Thy-1 minigene promoter [29]. The two transgenes cosegregate in these mice. APP/PS1 mice were maintained on a C57BL/6 J genetic background and genotyped by PCR analysis of genomic DNA from tail biopsies. All animals were kept in standard animal cages under conventional laboratory conditions (12 h light/dark cycle, 22 °C) with ad libitum access to food and water. The animals were randomized for therapy trials and coded, and the operators remained double-blinded to which treatment they received, until the completion of data collection. Male APP/PS1 transgenic mice and wild-type littermates were randomly assigned into four groups: TUDCA-treated and untreated (control) APP/PS1 mice, TUDCA-treated and untreated (control) wild-type mice. Animals were fed a diet of standard laboratory chow supplemented with either 0.4 % (wt/wt) TUDCA (sodium salt; Prodotti Chimici e Alimentari S.p.A., Basaluzzo, Italy), or no bile acid, custom made by Harlan (Harlan Laboratories Models, S.L., Barcelona, Spain). Treatment was started when the mice were 2 months old and continued for 6 months. The dose and duration of TUDCA, whose pharmacokinetics has been extensively studied in rodents [30], were chosen based on pilot studies using APP/PS1 mice and other animal studies [31]. The use of 2-month-old APP/PS1 mice to receive TUDCA treatment was based on previous reports demonstrating that amyloid deposits in this model start at 2–3 months and cognitive deficits are absent until 8 months [29].

Contextual Fear Conditioning After TUDCA treatment for 6 months, contextual fear conditioning experiments were

performed as described before [32]. Briefly, on day 1, mice were habituated for 5 min inside a sound attenuated box by placing them in a test chamber (26×22×18 cm) fitted with a grid floor to deliver electric shocks by a constant current shocker (Startle & fear combined, Panlab SLU, Harvard Apparatus, Barcelona, Spain). Movements were recorded online by a weight transducer system. On day 2, after 2 min of baseline recording, animals were conditioned to tone presentations (30 s, 4 kHz, 80 dB, inter-stimulus interval 60 s), co-terminated with a mild foot shock (2 s, 0.3 mA). Twenty-four hours later, retention to either context or tone (in a novel context) was assessed in two separate sessions. For contextual fear memory, animals were placed for 5 min in the conditioning context, and freezing was assessed as readout for retention memory. For cue-related memory retention, animals were tested in a novel context (context 2). Animals were placed for 6 min in context 2 (altered in tactile, olfactory and visual dimensions), and freezing to context 2 or to tone (3 min) was recorded. To compare contextual retention memory, freezing levels during contextual exposure were expressed in relation to acquisition levels (100 %) using the following formula: [(Freezing context/Freezing acquisition) − 1]×100. Values >0 indicate increased retention memory compared to freezing acquisition, while values <0 indicate reduced retention memory compared to conditioning.

Immunohistochemistry After behavior testing, animals were sacrificed by cervical dislocation, and the brain was removed. One hemisphere of the brain was snap-frozen for protein and RNA extraction. The other hemisphere was fixed and stored in 4 % paraformaldehyde in phosphate-buffered saline (PBS) and later dehydrated, treated with xylene, and embedded in paraffin. Serial 4-μm-thick coronal brain sections were cut on a microtome and mounted on SuperFrost-Plus (Thermo Scientific, Rockford, IL, USA) glass slides. Paraffin-embedded brain sections were deparaffined, rehydrated, and boiled three times in 10 mM citrate buffer, pH 6. Sections were then incubated for 60 min in blocking buffer [10 % (*v*/*v*) normal donkey serum (Jackson ImmunoResearch Laboratories Inc., West Grove, PA, USA) in PBS containing 0.1 % (*v*/*v*) Triton X-100 (Sigma-Aldrich, St. Louis, MO, USA)] and subsequently in appropriately diluted primary antibodies overnight at 4 °C. After rinsing, the primary antibody was developed by incubating with cyanine 2 (Cy2, Jackson)- or Alexa Fluor 594 (Invitrogen, Grand Island, NY, USA)-conjugated secondary antibodies against the corresponding species for 1 h at room temperature. The following primary antibodies were used for immunohistochemistry: Aβ plaques were immunostained with a mouse monoclonal anti-Aβ (6E10; Signet Laboratories Inc., Dedham, MA, USA; 1:1,000); astrocytes were stained with a mouse monoclonal glial fibrillary acidic protein (GFAP) antibody (GA5; Millipore Corporation, Temecula, CA, USA; 1:400); microglia were stained with a rabbit polyclonal Iba-I antibody (Wako Pure Chemicals, Richmond, VA, USA; 1:100); neuronal cell bodies and dendrites were labeled with a rabbit polyclonal microtubule associated protein 2 (MAP2) antibody (Millipore; 1:100); presynaptic terminals were labeled with a mouse monoclonal synaptophysin (SYN) antibody (SY38; Millipore; 1:100); neuronal nuclei were labeled with a mouse monoclonal neuronal nuclei (NeuN) antibody (A60; Millipore; 1:50). On control sections, where primary antibody was replaced by blocking buffer, no staining was observed (data not shown).

Histochemistry Paraffin-embedded brain sections were deparaffined, rehydrated, and stained with Thioflavin T (Sigma), a general marker of amyloid deposits. Incubation with freshly filtered 0.05 % Thioflavin T solution in PBS was performed for 8 min at room temperature [33].

Image Analysis and Semiquantification of Immunofluorescence Images were acquired with an Axioskop fluorescence microscope (Carl Zeiss GmbH, Hamburg, Germany). Semiquantitative analysis of mean fluorescence intensities (MFIs) of GFAP, Iba-I, and MAP2 was performed using NIH Image J software. Eight images of slides were obtained per hippocampal and cortical regions. Images were converted into an 8-bit format, and the background was subtracted. An intensity threshold was set and kept constant for all images analyzed. MFI per square millimeter area was calculated by dividing the MFI units by the area of outlined regions and is presented as a bar graph. The total number of thioflavin- and Aβ-positive plaques in the hippocampus and frontal cortex was counted and presented as plaque number per square millimeter.

Real-Time PCR Total RNA from dissected hippocampus and frontal cortex was isolated with TRIzol (Invitrogen), according to the manufacturer's instructions. Samples were homogenized in TRIzol using a motor-driven Bio-vortexer (No1083; Biospec Products, Bartlesfield, OK) and disposable RNAse/DNAse-free sterile pestles (Thermo Scientific). RNA was quantified using a NanoDrop spectrophotometer and typically showed A260/280 ratios between 1.9 and 2.1. cDNA was made using Superscript II Reverse Transcriptase (Invitrogen) according to the manufacturer's instructions.

Real-time quantitative PCR analysis was performed in the 7300 Real-Time PCR System (Applied Biosystems, Foster City, CA, USA), using SYBR Green PCR master mix (Fermentas International Inc., Glen Burnie, Maryland, USA) [34]. Triplicate reactions were run per sample. The expression levels relative to GAPDH were calculated using the $\Delta\Delta C_t$ method. TUDCA-untreated wild-type mice were used as the calibrator. The *n*-fold change in expression was obtained using the formula: $2^{-\Delta\Delta Ct}$ [35]. Primer sequences are presented in Table 1.

Western Blot Analysis Total protein extracts from dissected hippocampus and frontal cortex were prepared in lysis buffer, following standard protocols. Protein concentrations were determined using the Bio-Rad protein assay kit, according to the manufacturer's specifications. Sixty micrograms of total protein extracts was separated on 6 and 12 % sodium dodecyl sulfate–polyacrylamide gel electrophoresis. After electrophoretic transfer onto nitrocellulose membranes and blocking with a 5 % milk solution, membranes were incubated overnight at 4 °C with the following primary antibodies: rabbit polyclonal antibody reactive to CTGF (Abcam, Cambridge, UK), rabbit polyclonal antibody reactive to APOE (Santa Cruz Biotechnology, Santa Cruz, CA, USA), rabbit polyclonal antibody reactive to SORLA (Santa Cruz), and rabbit polyclonal antibody reactive to A2M (Santa Cruz). Finally, secondary goat anti-mouse or anti-rabbit IgG antibody conjugated with horseradish peroxidase (BioRad Laboratories, Hercules, CA, USA) was added for 3 h at room temperature. The membranes were processed for protein detection using the SuperSignal substrate (Pierce Biotechnology, Rockford, IL, USA). β-Actin (AC-15; Sigma-Aldrich) was used as loading control. The relative intensities of protein bands were analyzed using the QuantityOne Version 4.6 densitometric analysis program (Bio-Rad) and normalized to the respective loading control.

γ-Secretase Activity Assessment of γ-secretase activity was performed by detection of the ~7-kDa CTF-γ cleavage product of APP [14]. Briefly, 60 μg of total protein extracts was resolved electrophoretically in 10–20 % Tris–Tricine gels (Bio-Rad) and CTF-γ (and CTF-β) identified using an anti-APP, C-terminal rabbit polyclonal antibody (Sigma-Aldrich; 1:2,000). After stripping, membranes were incubated with the primary mouse monoclonal antibody reactive to soluble APP-β fragment with the Swedish mutation (sAPP-β; 6A1; Immuno-Biological Laboratories, Inc, Minneapolis, MN, USA; 5 μg/mL) and with the primary mouse monoclonal antibody reactive to Aβ (6E10; Signet; 1:1,000) to detect total Aβ peptide. Immunoreactivities were visualized as described above.

Sandwich ELISA Total protein extracts from dissected hippocampus and frontal cortex were used to determine Aβ concentration. Total $A\beta_{1-40}$ or $A\beta_{1-42}$ content was measured by sandwich ELISA (Millipore) according to the manufacturer's instructions. Wild-type animals were used as controls. Values were normalized to the respective total protein concentration and expressed as percentage of wild-type control.

Statistical Analysis Data were analyzed by the one-way analysis of variance (ANOVA), and differences between groups were determined by post hoc Bonferroni's test (Prism 2.01; GraphPad Software, Inc., San Diego, CA, USA). Comparison of data from two groups was made by Student's two-tailed unpaired *t* test. Values of $p<0.05$ were considered significant.

Results

TUDCA Prevents Aβ Plaque Accumulation in APP/PS1 Mice

Mutations of APP and PS1, as observed in APP/PS1 double transgenic mice, lead to an increase in Aβ production and deposition [29, 36–38]. In this study, we investigated the effect of TUDCA on Aβ deposition in the brains of wild-type and APP/PS1 mice. A general histological evaluation of amyloid plaque burden was performed with thioflavin. Thioflavin staining demonstrated a clear abundance of amyloid plaques in the brains of control transgenic mice, whereas deposits were absent in both control and TUDCA-treated wild-type mice (Fig. 1a). Importantly, a marked reduction of thioflavin plaque number was observed in hippocampus and frontal cortex of transgenic mice treated with TUDCA compared to control transgenic mice ($p<0.01$)

Table 1 Sense and antisense primers used to amplify each cDNA of interest

	Sense primer (5′–3′)	Antisense primer (5′–3′)
Mouse CTGF	AGCCTCAAACTCCAAACACC	CAACAGGGATTTGACCAC
Mouse A2M	CTCAGCACCACAGAAACCAA	ATGAAGGAGGCACAGTGGAA
Mouse APOE	TGTTTCGGAAGGAGCTGACT	TGTGTGACTTGGGAGCTCTG
Mouse SORLA	TAGCCTGGGAAGCCCAGC	TGGCAGCTTCCAGAGGTACAC
Mouse GAPDH	CATTGTGGAAGGGCTCATGAC	GCCCCACGGCCATCA

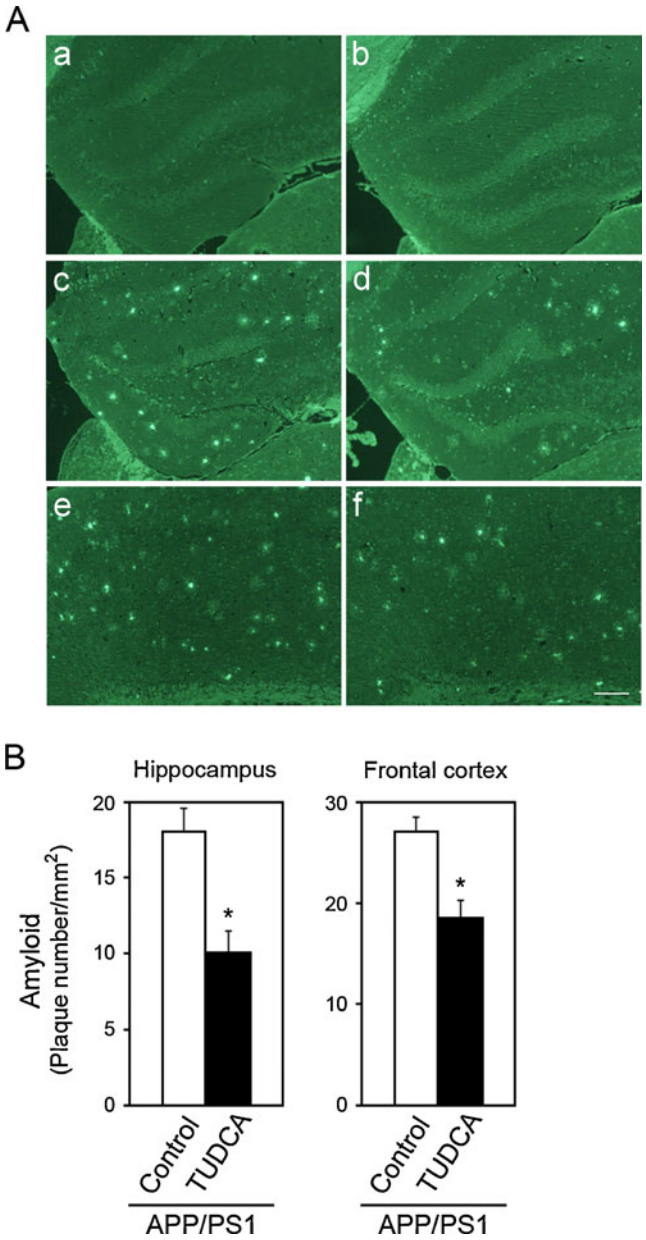

Fig. 1 TUDCA-treated APP/PS1 mice exhibit reduced levels of amyloid deposits compared with control APP/PS1 mice. **a** Representative images of thioflavin staining in the hippocampus of control (*a*) or TUDCA-treated (*b*) wild-type mice and in control (*c*) or TUDCA-treated (*d*) APP/PS1 mice, as well as in the frontal cortex of control (*e*) or TUDCA-treated (*f*) APP/PS1 mice. *Scale bar*, 50 μm. **b** Quantification of amyloid plaque number per square millimeter in hippocampus and frontal cortex of TUDCA-treated and untreated APP/PS1 mice. Values are from at least four images per animal. Data are mean ± SEM from 12–15 mice in each group. *$p<0.01$ from control APP/PS1 mice

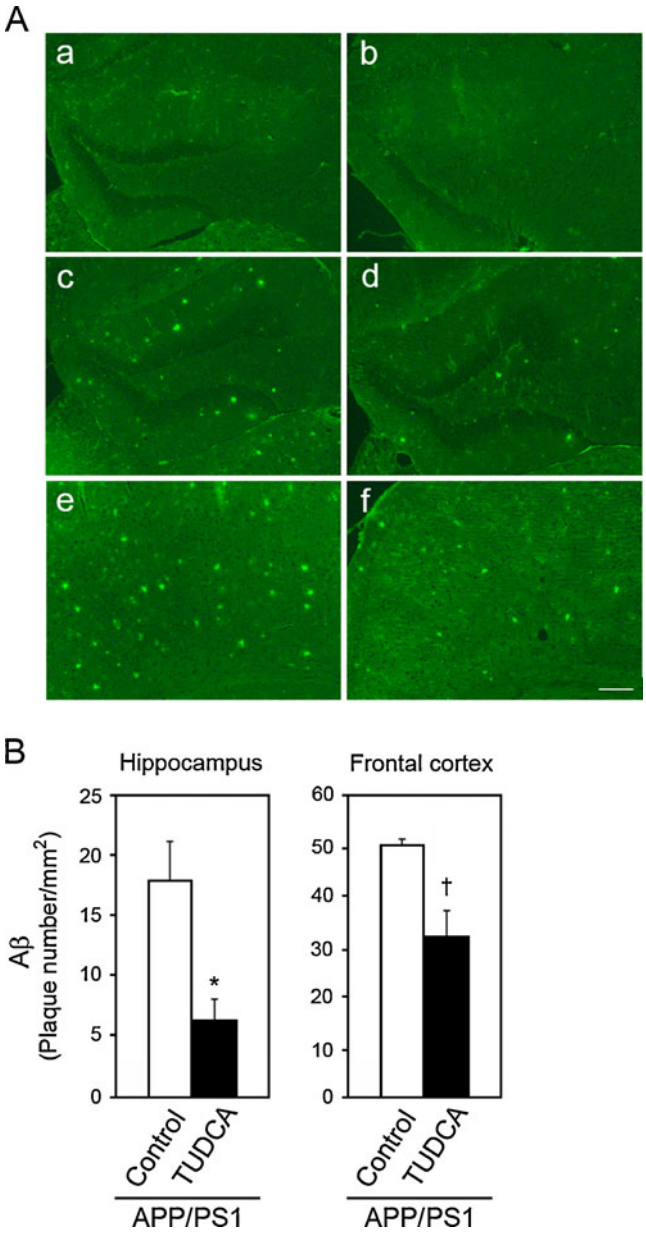

Fig. 2 TUDCA treatment results in decreased Aβ deposits in the brains of APP/PS1 mice compared with untreated APP/PS1 mice. **a** Representative images of Aβ immunostaining in the hippocampus of control (*a*) or TUDCA-treated (*b*) wild-type mice and in control (*c*) or TUDCA-treated (*d*) APP/PS1 mice, as well as in the frontal cortex of control (*e*) or TUDCA-treated (*f*) APP/PS1 mice. *Scale bar*, 50 μm. **b** Quantification of Aβ plaque number per millimeter in hippocampus and frontal cortex of TUDCA-treated and untreated APP/PS1 mice. Values are from at least four images per animal. Data are mean ± SEM from 12–15 mice in each group. *$p<0.01$ and †$p<0.05$ from control APP/PS1 mice

(Fig. 1a and b). Aβ immunohistochemistry confirmed the presence of Aβ deposits in APP/PS1 transgenic mice, but not in wild-type mice (Fig. 2a). Furthermore, Aβ plaque number was strongly decreased by almost 65 % in the hippocampus and 40 % in the frontal cortex of TUDCA-treated APP/PS1 mice compared with untreated transgenic mice ($p<0.01$ and $p<0.05$, respectively) (Fig. 2a and b). These results demonstrate that TUDCA treatment

significantly attenuates Aβ levels in both the hippocampus and frontal cortex of APP/PS1 transgenic mice, suggesting an inhibitory effect of TUDCA on Aβ deposition.

TUDCA Inhibits Activation of Astrocytes and Microglia in APP/PS1 Mice

In the brains of human AD patients and transgenic AD mouse models, activation of astrocytes and microglia is observed in the area of Aβ plaques [29, 39, 40], contributing to an inflammatory process that develops around injury in the brain [41]. To investigate whether TUDCA prevents this potentially neurotoxic, inflammatory response, we compared astrocytic and microglial reactivity in TUDCA-treated and untreated APP/PS1 and wild-type mice. Activated astrocytes were visualized by GFAP immunofluorescence. GFAP staining demonstrated a marked increase of reactive astrocytes in the brains of control transgenic mice compared to wild-type mice ($p<0.01$) (Fig. 3a and b). In contrast, GFAP immunoreactivity was decreased in both hippocampus and frontal cortex of TUDCA-treated APP/PS1 mice ($p<0.05$) (Fig. 3a and b). Activated microglia were visualized by Iba-I immunostaining. As shown in Fig. 4, a significant elevation of Iba-I immunoreactivity was observed in control APP/PS1 mice compared to wild-type mice ($p<0.01$). Noteworthy, significantly less Iba-I immunoreactivity was observed in TUDCA-treated APP/PS1 mice relative to control APP/PS1 mice ($p<0.05$) (Fig. 4a and b). To visualize the reactive microglia surrounding amyloid plaques, sections were stained with thioflavin after Iba-I immunofluorescence. Double-staining of Iba-I and amyloid plaques showed accumulation of reactive microglia around the plaques in the brains of control APP/PS1 mice, whereas fewer reactive microglia were observed around the less amyloid plaques in the brains of TUDCA-treated APP/PS1 mice (Fig. 4c). NF-κB, a known marker of inflammation, increased in control APP/PS1 mice compared to wild-type animals and decreased in TUDCA-treated APP/PS1 mice relative to control APP/PS1 mice (data not shown). These results suggest that inflammation is modulated by TUDCA in APP/PS1 mice.

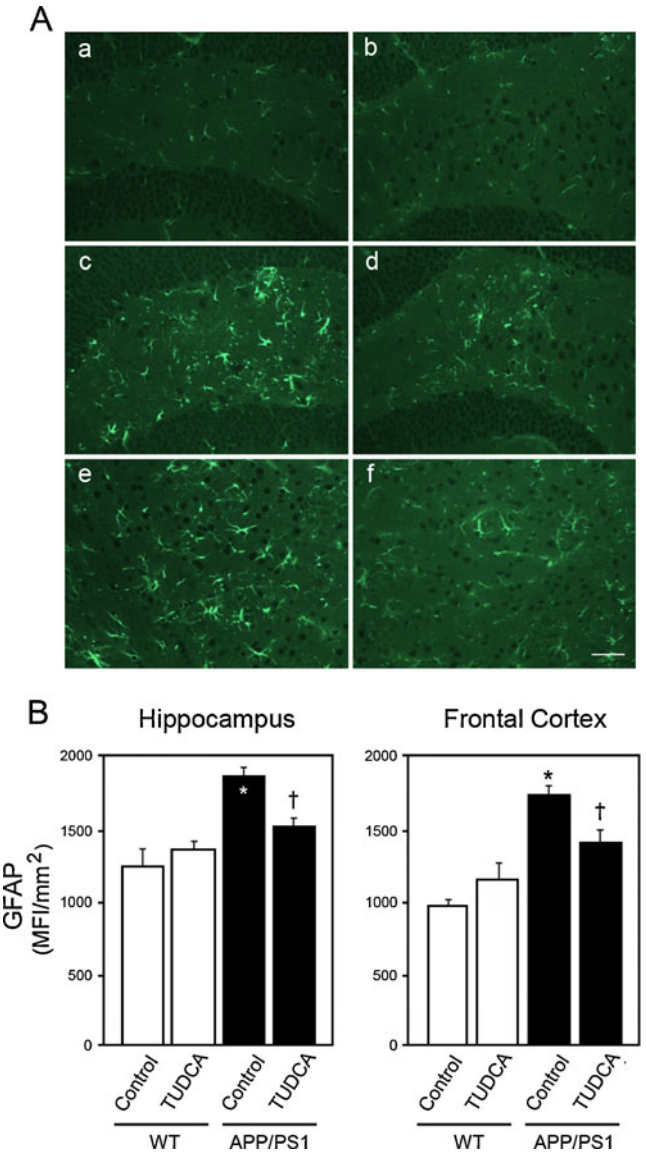

Fig. 3 TUDCA treatment decreases astrocytic activation in the brains of APP/PS1 mice. **a** Representative images of GFAP immunostaining in the hippocampus of control (*a*) or TUDCA-treated (*b*) wild-type mice and in control (*c*) or TUDCA-treated (*d*) APP/PS1 mice, as well as in the frontal cortex of control (*e*) or TUDCA-treated (*f*) APP/PS1 mice. *Scale bar*, 25 μm. **b** Quantification of GFAP mean fluorescent intensity (*MFI*) per square millimeter in hippocampus and frontal cortex of TUDCA-treated or untreated wild-type and APP/PS1 mice. Values are from at least eight images per animal. Data are mean ± SEM from 12–15 mice in each group. *$p<0.01$ from control wild-type mice and †$p<0.05$ from control APP/PS1 mice

TUDCA Prevents Loss of Neuronal Integrity in APP/PS1 Mice

Neuronal degeneration and loss observed in the brains of AD patients [42] and in the brains of APP/PS1 transgenic mice [29, 43, 44] is hypothesized to be exacerbated by an inflammatory reaction [41]. Given the inhibitory effect of TUDCA on glial activation, we examined the levels of the neuronal marker MAP2, expressed on neuronal cell bodies and dendrites, in the brains of wild-type and APP/PS1 mice treated or untreated with TUDCA. Consistent with previous reports showing decreased MAP2 immunoreactivity in the hippocampus of APP/PS1 mice [43], our results showed that control APP/PS1 mice displayed significantly less brain MAP2 immunoreactivity when compared to wild-type mice ($p<0.01$) (Fig. 5a and b). Importantly, TUDCA treatment prevented the loss on MAP2 immunoreactivity in both the

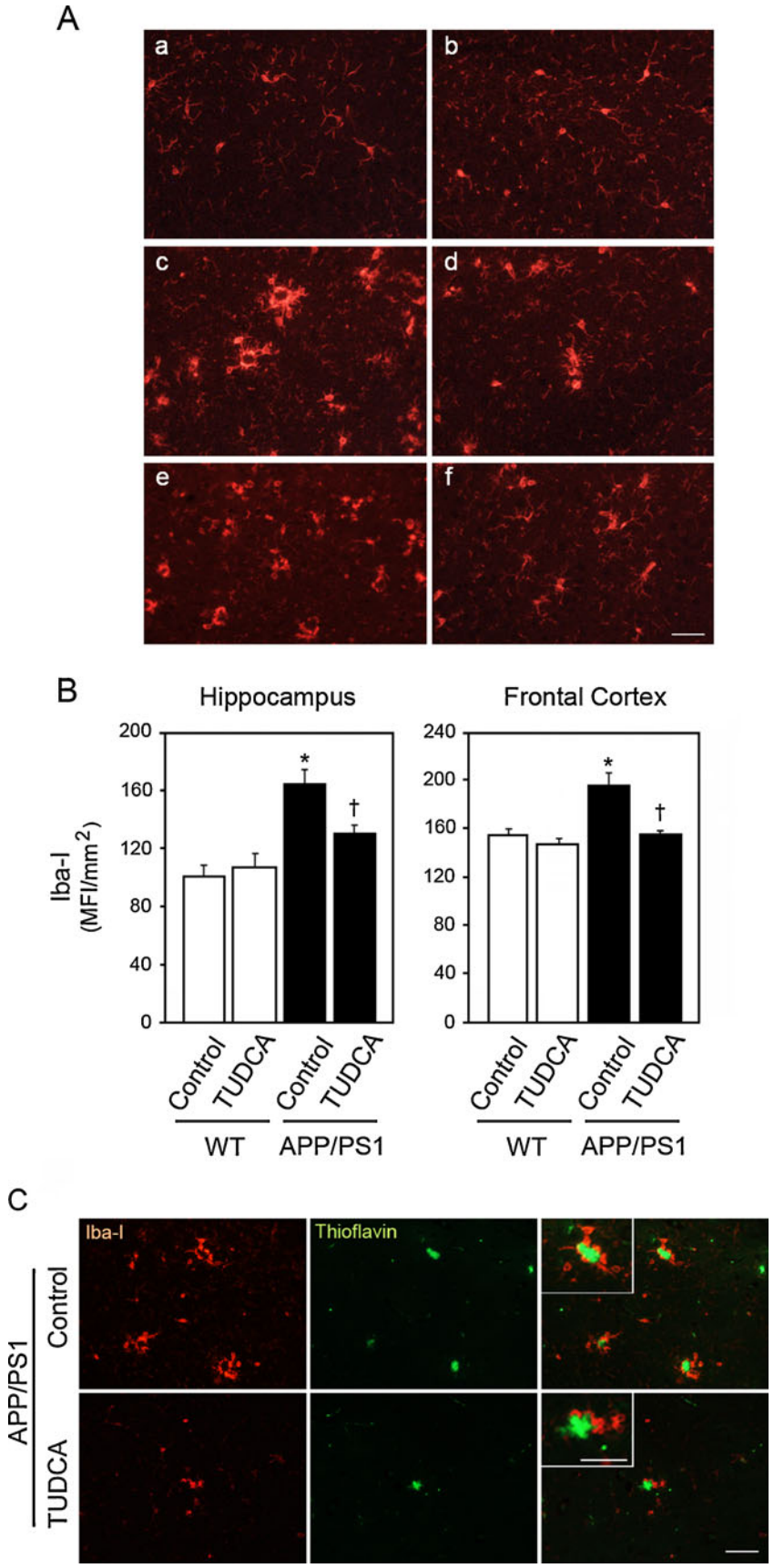

Fig. 4 TUDCA treatment decreases microglial activation in the brains of APP/PS1 mice. **a** Representative images of Iba-I immunostaining in the hippocampus of control (*a*) or TUDCA-treated (*b*) wild-type mice and in control (*c*) or TUDCA-treated (*d*) APP/PS1 mice, as well as in the frontal cortex of control (*e*) or TUDCA-treated (*f*) APP/PS1 mice. Scale bar, 25 μm. **b** Quantification of Iba-I mean fluorescent intensity (*MFI*) per square millimeter in hippocampus and frontal cortex of TUDCA-treated or untreated wild-type and APP/PS1 mice. Values are from at least eight images per animal. Data are mean ± SEM from 12–15 mice in each group. *$p<0.01$ from control wild-type mice and †$p<0.05$ from control APP/PS1 mice. **c** Double staining of Iba-I and amyloid plaques (thioflavin staining) in the hippocampal region of TUDCA-treated and untreated APP/PS1 mice. *Scale bar*, 25 μm

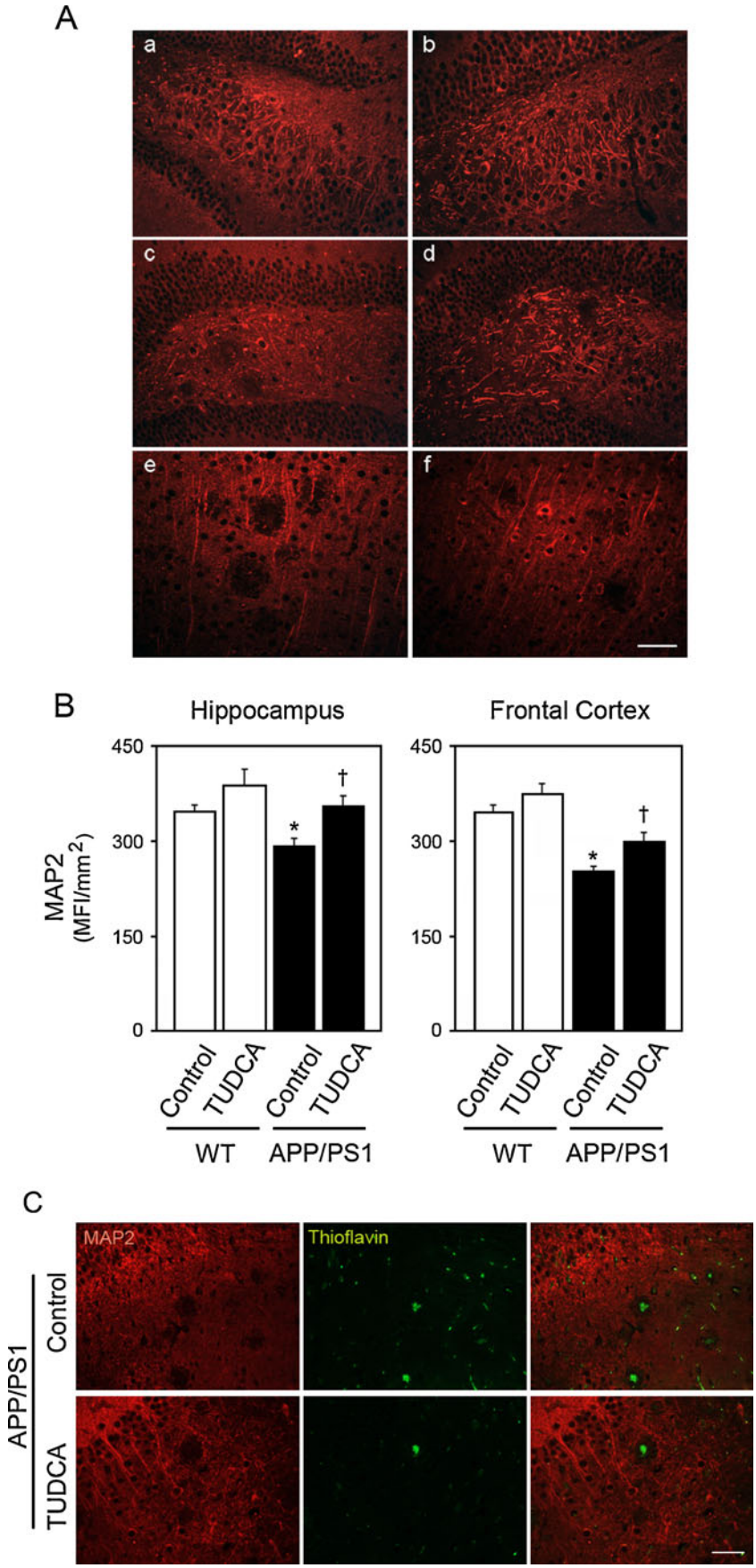

Fig. 5 TUDCA treatment prevents neuronal integrity loss in the brains of APP/PS1 mice. **a** Representative images of MAP2 immunostaining in the hippocampus of control (*a*) or TUDCA-treated (*b*) wild-type mice and in control (*c*) or TUDCA-treated (*d*) APP/PS1 mice, as well as in the frontal cortex of control (*e*) or TUDCA-treated (*f*) APP/PS1 mice. *Scale bar*, 25 μm. **b** Quantification of MAP2 mean fluorescent intensity (*MFI*) per square millimeter in hippocampus and frontal cortex of TUDCA-treated or untreated wild-type and APP/PS1 mice. Values are from at least eight images per animal. Data are mean ± SEM from 12–15 mice in each group. *$p<0.01$ from control wild-type mice and †$p<0.05$ from control APP/PS1 mice. **c** Double staining of MAP2 and amyloid plaques (thioflavin staining) in the hippocampal region of TUDCA-treated and untreated APP/PS1 mice. *Scale bar*, 25 μm

hippocampus and frontal cortex of APP/PS1 mice ($p<0.05$) (Fig. 5a and b). Double staining of MAP2 and amyloid plaques showed a considerable degeneration of neurons, characterized by damage or loss of neuronal fibers surrounding amyloid plaques in the brains of control APP/PS1 mice (Fig. 5c). In contrast, a significant improvement in the integrity of the neuronal fibers was observed around the less amyloid plaques in the brains of TUDCA-treated APP/PS1 mice. Similar results were observed with the neuronal marker SYN, which labels presynaptic terminals, and the neuron-specific nuclear protein NeuN (Fig. 6a, b and c). As depicted in low-magnification images of NeuN immunostaining, the decreased neuronal staining in CA1, CA3 and dentate gyrus of APP/PS1 mice hippocampus was partially rescued by TUDCA treatment (Fig. 6a). These data suggest that TUDCA treatment decreases the rate of neuronal degeneration in APP/PS1 mice.

TUDCA Modulates Lipid Metabolism Mediators in APP/PS1 Mice

Given the effect of TUDCA in regulating the expression of lipid-metabolism mediators in hepatocytes [27] and the role of lipid mediators in modulating Aβ metabolism [15], we assessed CTGF, A2M, APOE, and SORLA levels in the brains of wild-type and APP/PS1 mice treated and untreated with TUDCA. Quantitative real-time PCR analysis demonstrated increased expression of CTGF, A2M, and APOE in the hippocampus and frontal cortex of control APP/PS1 mice compared to wild-type mice ($p<0.05$ and $p<0.01$), whereas a trend for decreased expression of SORLA in APP/PS1 mice was observed in both cerebral regions (Fig. 7a and b). In agreement with the microarray gene expression profile in hepatocytes and a potential neuroprotective mechanism for TUDCA, this bile acid significantly decreased CTGF, A2M, and APOE expression in APP/PS1 mice hippocampus ($p<0.05$), while slightly increasing SORLA expression (Fig. 7a). In the frontal cortex, only CTGF expression was significantly decreased by TUDCA treatment of APP/PS1 mice ($p<0.05$), although a trend for decreased A2M and APOE expression was also observed (Fig. 7b). Similar results were obtained at the protein level by Western blot analysis of total protein extracts from hippocampus (Fig. 8a) and frontal cortex (Fig. 8b). These results indicate that TUDCA regulates the levels of lipid-metabolism mediators involved in Aβ production and accumulation.

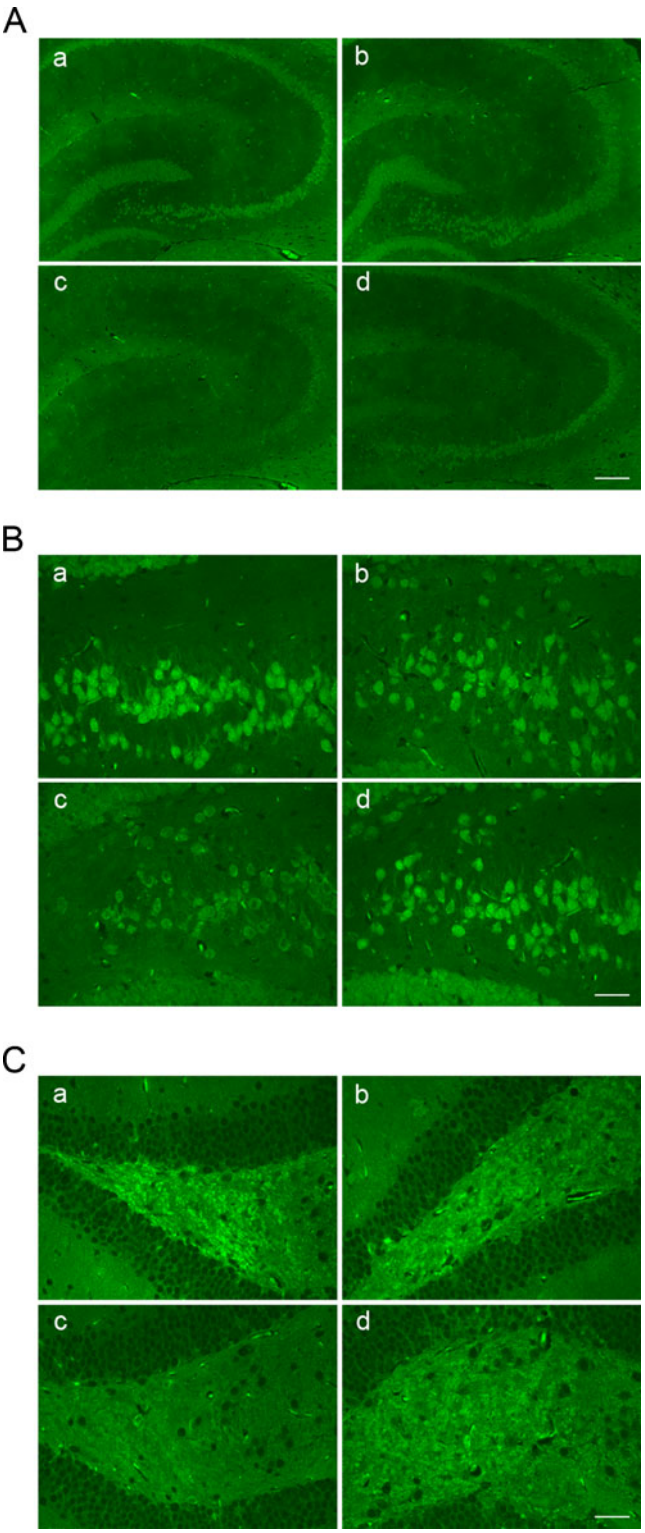

Fig. 6 TUDCA treatment prevents loss of NeuN and SYN immunoreactivity in the brains of APP/PS1 mice. **a** Representative low-magnification images of NeuN immunostaining in the hippocampus of control (a) or TUDCA-treated (b) wild-type mice and in control (c) or TUDCA-treated (d) APP/PS1 mice. *Scale bar*, 50 μm. **b** Representative images of NeuN immunostaining in the hippocampus of control (a) or TUDCA-treated (b) wild-type mice and in control (c) or TUDCA-treated (d) APP/PS1 mice. *Scale bar*, 25 μm. **c** Representative images of SYN immunostaining in the hippocampus of control (a) or TUDCA-treated (b) wild-type mice and in control (c) or TUDCA-treated (d) APP/PS1 mice. *Scale bar*, 25 μm

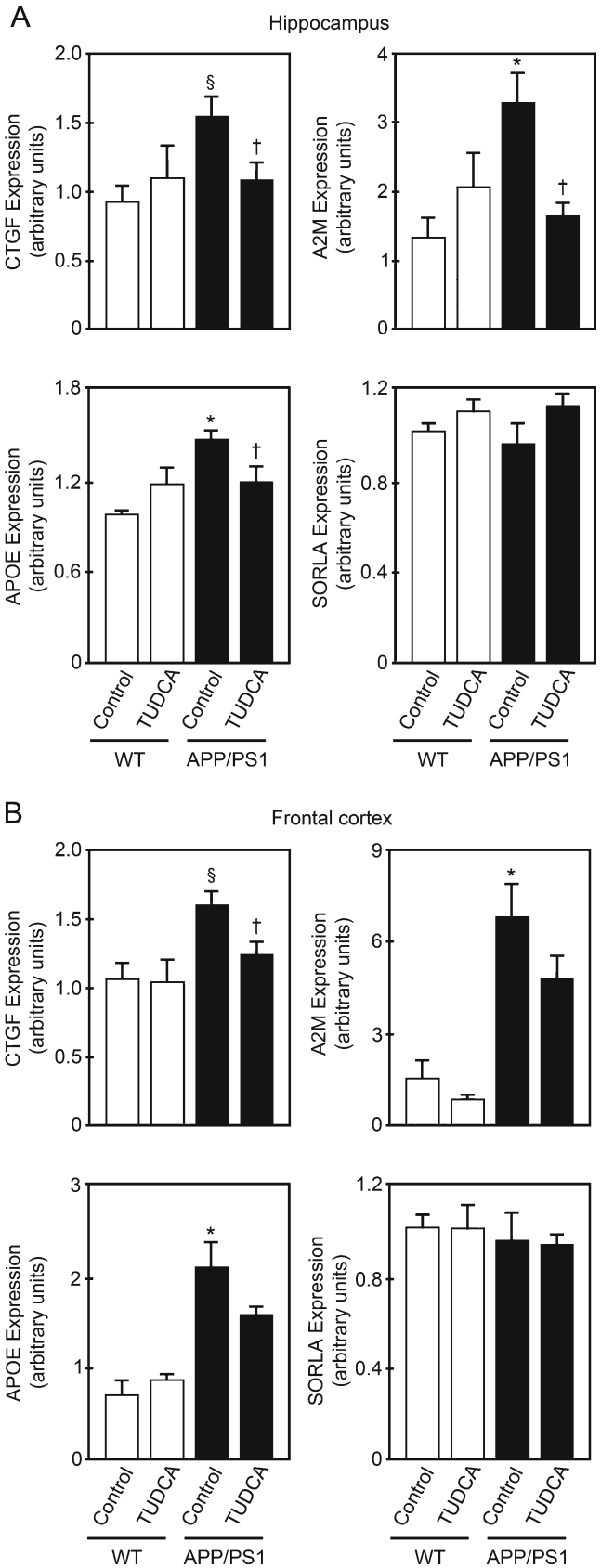

Fig. 7 TUDCA regulates the expression of lipid-metabolism mediators associated with AD pathology in the brains of APP/PS1 mice. Quantification of CTGF, A2M, APOE, and SORLA mRNA levels in the **a** hippocampus and **b** frontal cortex of TUDCA-treated or untreated wild-type and APP/PS1 mice, by real-time PCR. Data are mean ± SEM from 12–15 mice in each group. §$p<0.05$ and *$p<0.01$ from control wild-type mice and †$p<0.05$ from control APP/PS1 mice

TUDCA Prevents APP Processing and Aβ Production in APP/PS1 Mice

Having established the ability of TUDCA in modulating brain lipid-metabolism mediators involved in Aβ metabolism, we hypothesized that decreased amyloidogenic processing of APP is the mechanism underlying the diminished amyloid pathology in TUDCA-fed APP/PS1 mice. To determine whether TUDCA influences γ-secretase activity, brain tissues from untreated and TUDCA-treated APP/PS1 mice or wild-type littermates were subjected to electrophoresis in 10–20 % Tris–Tricine gels, followed by immunoblot analysis of APP-CTF-γ using an anti-APP-CTF antibody, which also recognizes full-length APP. A decrease in the production of CTF-γ was observed in TUDCA-treated APP/PS1 mice compared to control transgenic mice, whereas full-length APP levels remained unchanged (Fig. 9). These findings suggest that TUDCA influences APP processing via modulation of γ-secretase activity. Curiously, CTF-β and sAPP-β fragment were also found decreased in TUDCA-fed transgenic mice compared to control transgenic mice (Fig. 9). In agreement with the decreased CTF-γ and CTF-β, total Aβ levels were also decreased in TUDCA-treated APP/PS1 mice compared to control APP/PS1 mice (Fig. 9). These results point toward a reduction in overall amyloidogenic APP processing with TUDCA treatment.

To further corroborate that TUDCA-mediated decrease in APP processing impacts on Aβ generation, we analyzed Aβ levels in the hippocampus and frontal cortex of untreated and TUDCA-treated wild-type and APP/PS1 brains by sandwich ELISA. Consistent with others [29, 36–38], our results showed a dramatic increase in $A\beta_{1-40}$ and $A\beta_{1-42}$ levels in the brains of control APP/PS1 mice, with $A\beta_{1-42}$ exceeding $A\beta_{1-40}$ by ~10-fold (Fig. 10a and b). $A\beta_{1-42}$ to $A\beta_{1-40}$ ratio, known to be positively correlated with AD pathology [45], was also strongly increased by ~15-fold in control transgenic mice compared to wild-type mice (data not shown). Importantly, TUDCA treatment significantly decreased $A\beta_{1-40}$ and $A\beta_{1-42}$ levels in both hippocampus and frontal cortex of APP/PS1 mice ($p<0.01$) (Fig. 10a and b), suggesting that TUDCA interferes with Aβ production, possibly through the regulation of lipid-metabolism mediators associated with APP processing.

TUDCA Rescues Cognitive Deficits in APP/PS1 Mice

The APP/PS1 AD mouse model is well-known to develop Aβ-associated cognitive deterioration with increasing age

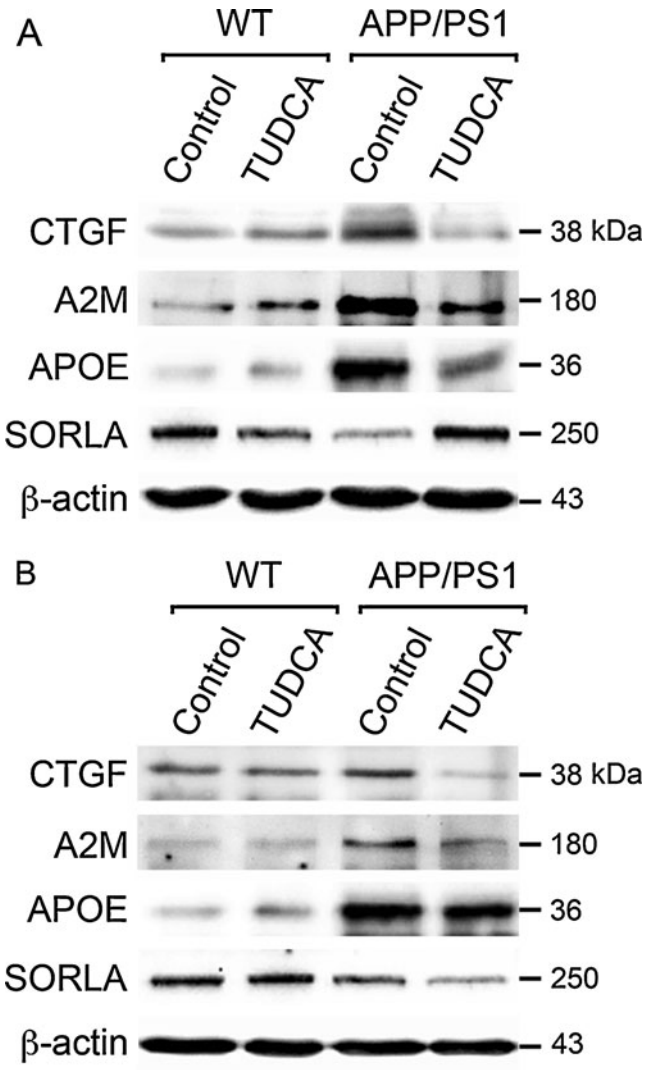

Fig. 8 TUDCA modulates protein levels of lipid-metabolism mediators associated with AD pathology in the brains of APP/PS1 mice. Representative immunoblots of CTGF, A2M, APOE, and SORLA in **a** hippocampal and **b** frontal cortex lysates of wild-type and APP/PS1 mice treated and untreated with TUDCA. β-Actin was used as loading control. Immunoblots are representative of 12–15 mice in each group

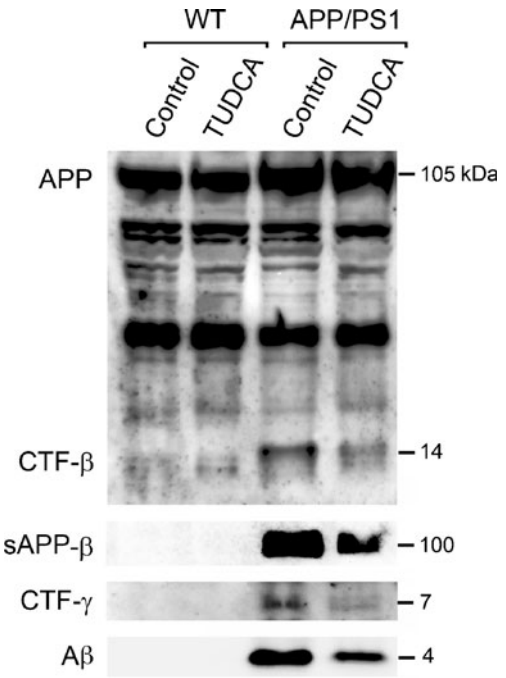

Fig. 9 TUDCA treatment decreases the production of APP–CTFs and Aβ in the brains of APP/PS1 mice. Representative immunoblots of CTF-γ, CTF-β, sAPP-β, and total Aβ in brain lysates of wild-type and APP/PS1 mice treated and untreated with TUDCA. APP was used as a normalization protein. Immunoblots are representative of five mice in each group

[29]. To test whether TUDCA supplementation prevents the memory deficits developed by APP/PS1 transgenic mice, we performed the contextual fear conditioning test. No significant effect of genotype or drug was observed in contextual fear conditioning (context 1) on memory retention ($F3, 45=2.29$, n.s.) (Fig. 11a). This retention memory was specific to context 1 in all but APP/PS1 control group. While both wild-type groups and TUDCA-treated APP/PS1 mice showed significantly reduced freezing to context 2, APP/PS1 control mice showed unspecific (similar to conditioning) freezing. Comparison of retention memory in context 2 using a one-way ANOVA indicated a significant *group* effect ($p<0.001$). Post hoc comparisons indicated a significant difference between control wild-type and control APP/PS1 mice ($p<0.01$) and between control and TUDCA-supplemented APP/PS1 mice ($p<0.001$) (Fig. 11a). This indicates a poor discrimination between a conditioned context and a novel context in control APP/PS1 mice. This lack of discrimination is reversed in TUDCA-supplemented APP/PS1 mice. In comparison, auditory fear conditioning to the tone was similar in all groups (Fig. 11b). These findings suggest that TUDCA may prevent memory deficits in APP/PS1 mice, through the attenuation of Aβ-associated neurodegeneration.

Discussion

This is the first demonstration of the therapeutic effects of TUDCA on AD pathology in vivo, which suggests a novel approach in AD therapy. Our findings indicate that TUDCA treatment inhibits accumulation of Aβ deposits in cortical and hippocampal regions of APP/PS1 double-transgenic mice. TUDCA was also effective at reducing astrocytic and microglial activation, while increasing the levels of the neuronal markers MAP2, NeuN, and SYN. Importantly, TUDCA prevented $A\beta_{1-40}$ and $A\beta_{1-42}$ production in both hippocampus and frontal cortex of APP/PS1 mice, possibly through the regulation of lipid-metabolism mediators involved in APP processing. Finally, these observations

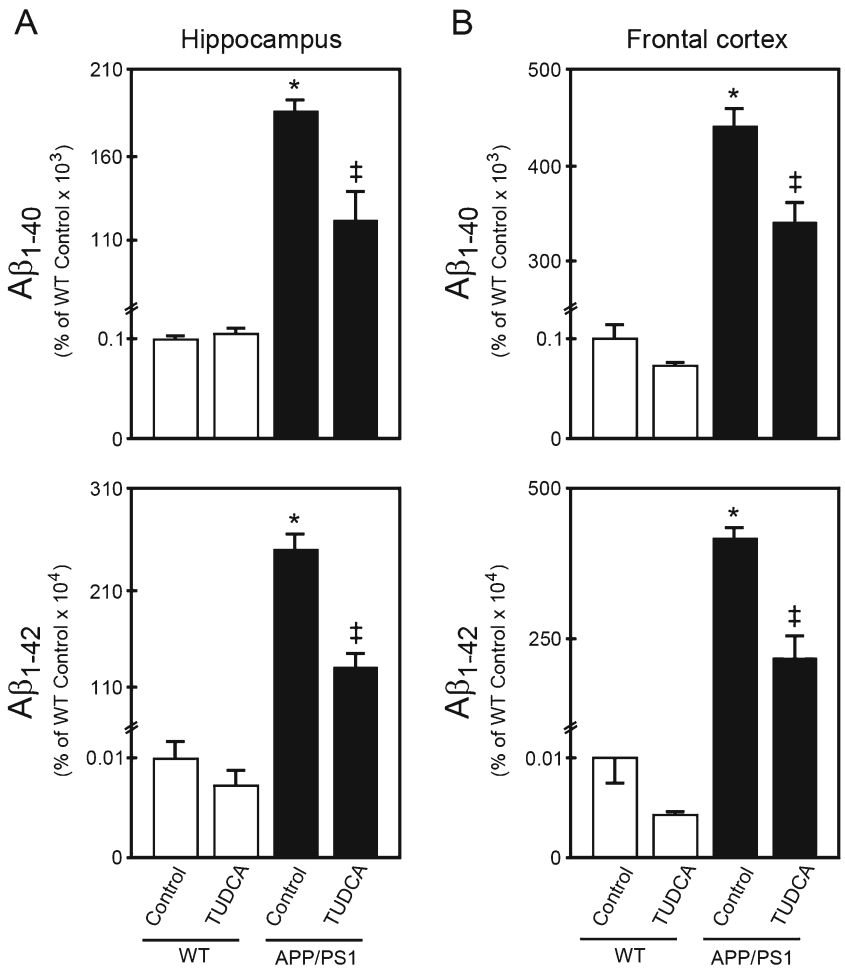

Fig. 10 TUDCA decreases $A\beta_{1-40}$ and $A\beta_{1-42}$ levels in the brains of APP/PS1 mice. Quantification of $A\beta_{1-40}$ and $A\beta_{1-42}$ levels in the **a** hippocampus and **b** frontal cortex of wild-type and APP/PS1 mice treated and untreated with TUDCA, by sandwich ELISA. Data are mean ± SEM from eight to ten mice in each group. *$p<0.01$ from control wild-type mice and ‡$p<0.01$ from control APP/PS1 mice

correlated with a clear rescue of memory deficits in TUDCA-treated APP/PS1 mice compared to control transgenic mice.

The inhibitory effect of TUDCA on the accumulation of Aβ deposits in APP/PS1 transgenic mice is likely attributable to its modulation of APP processing, as the production of amyloidogenic APP–CTF-γ and APP–CTF-β, direct precursors of Aβ was decreased by TUDCA treatment. The lack of TUDCA effect on Aβ peptide aggregation and secondary structure in vitro [26] further supports a role for TUDCA on Aβ production rather than on fibrillogenesis. APP processing can be modulated by different mechanisms, including but not limited to an altered function of γ-secretase [5]. Accordingly, γ-secretase activity, as assessed by the detection of APP–CTF-γ, was reduced in TUDCA-treated APP/PS1 mice. γ-Secretase generates the C terminus of Aβ from APP [5], and its selective modulation represents an attractive therapeutic strategy. Besides being an important drug target, γ-secretase is also involved in the regulation of key physiological processes, most notoriously Notch signaling [46]. As a therapeutic application, it is essential that TUDCA does not interfere with the cleavage of γ-secretase substrate Notch receptor, given the potential adverse effects of targeting this pathway [47]. Importantly, ongoing studies suggest that TUDCA does not inhibit the Notch signaling pathway (data not shown).

We have previously shown that bile acids modulate lipid metabolism gene expression [27]. In fact, TUDCA-treated hepatocytes revealed a strong downregulation of A2M and CTGF by >10-fold, in addition to other genes mainly involved in lipid and glucose metabolism. In this study, we confirmed in vivo that TUDCA downregulates CTGF and A2M in the brains of APP/PS1 mice. In addition to these regulators of lipid metabolism, we also show that APOE and, to a lesser extent, SORLA are modulated by TUDCA treatment of APP/PS1 transgenic mice. CTGF is an important player in AD pathogenesis as it regulates APP processing and Aβ production, presumably by increasing γ-secretase activity [14]. Consistent with increased CTGF levels in a mouse model of AD-type amyloid plaque burden and in AD brain [14], we observed a marked increase of CTGF levels in the brains of untreated APP/PS1 transgenic mice. Noteworthy, TUDCA-mediated decrease of CTGF levels was accompanied by a reduction of APP–CTF-γ levels, suggesting that modulation of γ-secretase activity may account, at least in part, for TUDCA neuroprotective

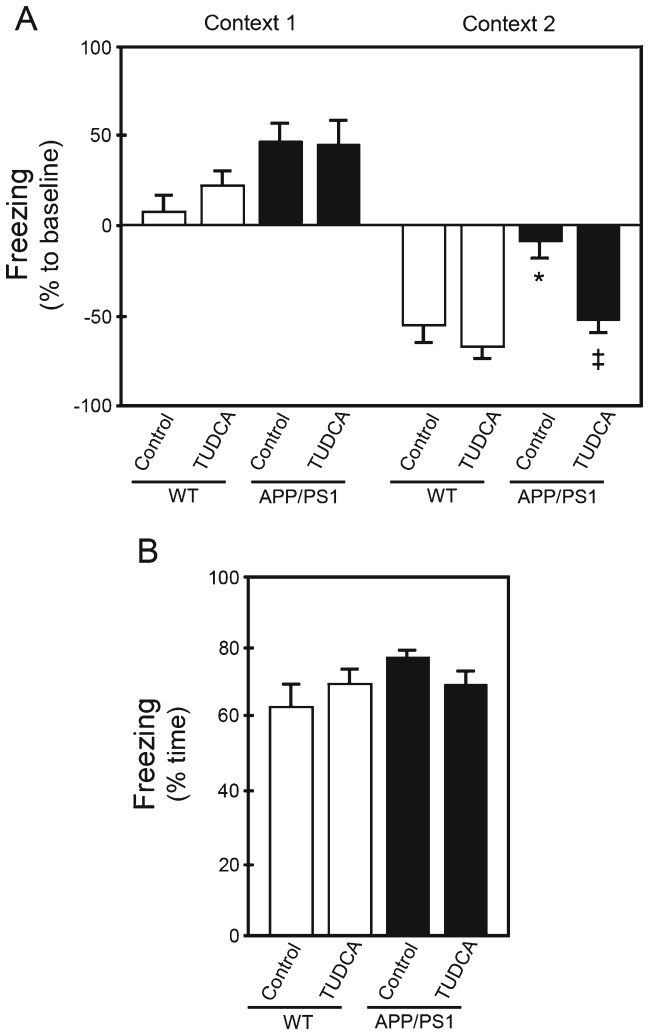

Fig. 11 TUDCA rescues memory deficits in APP/PS1 mice. **a** Contextual fear conditioning test of wild-type and APP/PS1 mice treated and untreated with TUDCA. Using freezing during acquisition as a reference, we measured the amount of freezing in both contexts. All groups showed similar freezing levels in context 1. In context 2, which was not associated with a shock, control APP/PS1 mice froze significantly more than other groups. Both wild-type groups and TUDCA-supplemented APP/PS1 mice recognized context 2 as a novel context and thus displayed decreased freezing. Data are calculated as percent change from acquisition levels and presented as mean ± SEM. **b** Auditory fear conditioning was similar in wild-type and APP/PS1 mice treated and untreated with TUDCA. Data are presented as mean ± SEM. *$p<0.01$ from control wild-type mice and ‡$p<0.001$ from control APP/PS1 mice

mechanism. In contrast with CTGF, SORLA plays a protective role in AD by reducing APP processing and Aβ generation [12]. Loss of SORLA occurs in AD brain patients [48]. Accordingly, we observed decreased SORLA protein levels in the hippocampus of control APP/PS1 mice. Importantly, TUDCA treatment of APP/PS1 mice significantly increased SORLA levels, which might explain the decreased levels of APP–CTF-β observed in TUDCA-fed transgenic animals. Each of these mechanisms in separate, or a combination of both, ultimately leads to decreased Aβ production. Accordingly, in this study, we demonstrate decreased Aβ levels in the brains of TUDCA-fed APP/PS1 mice, using different experimental approaches that included immunohistochemistry, ELISA, and immunoblot analysis. In addition to TUDCA modulation of lipid metabolism mediators involved in APP processing, the possibility of a direct interaction between TUDCA and presenilin, as recently reported for phenylpiperidine-type γ-secretase modulators [49], should be explored in future studies. APOE and A2M bind avidly to Aβ peptides and are found within amyloid plaques in AD mouse models and brain patients [50, 51]. Consistent with the abundance of Aβ plaques, APOE and A2M were found increased in APP/PS1 mice, whereas decreased levels were associated with fewer amyloid plaques in the brains of TUDCA-treated APP/PS1 animals.

Given the central role of Aβ plaques in the activation of microglia and astrocytes in AD brain [39] and AD animal models [29, 40], the significant decrease in activated microglia and astrocytes in TUDCA-treated APP/PS1 mice can be attributed to its inhibition of Aβ accumulation. However, TUDCA appears to possess an inherent anti-inflammatory function independent of Aβ [52, 53]. Although the underlying mechanisms remain unclear, TUDCA-mediated inhibition of endoplasmic reticulum stress may play a role in this process [52, 53]. Nevertheless, because brain inflammation is a risk factor for neurodegenerative disease, the anti-inflammatory effect of TUDCA in the APP/PS1 mouse model provides additional evidence for its therapeutic potential in AD.

In the brains of APP/PS1 mice, a discrete neuronal loss is associated with Aβ plaques [29, 44, 54]. Consistent with this result, we observed decreased immunoreactivity of neuronal markers MAP2, NeuN, and SYN in the hippocampus and frontal cortex of control APP/PS1 mice, indicating impaired neuronal integrity in these animals. Noteworthy, TUDCA treatment of APP/PS1 mice resulted in a clear rescue of neuronal marker immunoreactivity, suggesting that neuronal integrity loss observed in control APP/PS1 mice was prevented by TUDCA. Most degenerative neurons were observed around amyloid plaques in control APP/PS1 mice. In TUDCA-treated APP/PS1 mice, Aβ deposits were significantly less, and correspondingly, the extent of neuronal loss was much lower compared with control APP/PS1 mice. The neuroprotective effect of TUDCA in APP/PS1 mice is in line with previous reports showing protection against Aβ-induced neuronal toxicity [22–25] and also in other models of neurodegenerative diseases [18, 20].

In conclusion, our findings indicate that TUDCA treatment inhibits accumulation of Aβ deposits in APP/PS1 double-transgenic mice by decreasing Aβ production. Glial activation and neuronal integrity loss observed in untreated APP/PS1 mice were also prevented by TUDCA.

Importantly, TUDCA improved contextual fear memory in transgenic mice compared to untreated transgenic animals. This study clearly contributes to a better understanding of the cellular mechanisms that specifically regulate γ-secretase activity, Aβ load and AD pathology, and highlights TUDCA as a new, potent, and potentially more specific therapeutic approach.

Acknowledgments The authors thank Prodotti Chimici e Alimentari S. p.A. (Basaluzzo, Italy) for the supply of TUDCA. APP/PS1 mice were kindly donated by Bart De Strooper. We also wish to thank Véronique Hendrickx for assistance in genotyping the mice. This work was supported by grant PTDC/SAU-NMC/117877/2010 from Fundação para a Ciência e a Tecnologia (FCT), Portugal. AFN and JDA were recipients of postdoctoral fellowships (SFRH/BPD/34603/2007 and SFRH/BPD/47376/2008, respectively); RJV and MBF were recipients of Ph.D. fellowships (SFRH/BD/30467/2006 and SFRH/BD/43959/2008, respectively) from FCT. RDH and ACL were funded by 7FP grant MEMOSAD and the federal science fund FWO-Vlaanderen (grant number G.0327.08).

Conflict of interest The authors declare that they have no conflict of interest.

References

1. Selkoe DJ (2001) Alzheimer's disease: genes, proteins, and therapy. Physiol Rev 81:741–766
2. Goate A, Chartier-Harlin MC, Mullan M, Brown J, Crawford F, Fidani L, Giuffra L, Haynes A, Irving N, James L et al (1991) Segregation of a missense mutation in the amyloid precursor protein gene with familial Alzheimer's disease. Nature 349:704–706
3. Sherrington R, Rogaev EI, Liang Y, Rogaeva EA, Levesque G, Ikeda M, Chi H, Lin C, Li G, Holman K et al (1995) Cloning of a gene bearing missense mutations in early-onset familial Alzheimer's disease. Nature 375:754–760
4. Rogaev EI, Sherrington R, Rogaeva EA, Levesque G, Ikeda M, Liang Y, Chi H, Lin C, Holman K, Tsuda T et al (1995) Familial Alzheimer's disease in kindreds with missense mutations in a gene on chromosome 1 related to the Alzheimer's disease type 3 gene. Nature 376:775–778
5. De Strooper B, Saftig P, Craessaerts K, Vanderstichele H, Guhde G, Annaert W, Von Figura K, Van Leuven F (1998) Deficiency of presenilin-1 inhibits the normal cleavage of amyloid precursor protein. Nature 391:387–390
6. Edbauer D, Winkler E, Regula JT, Pesold B, Steiner H, Haass C (2003) Reconstitution of gamma-secretase activity. Nat Cell Biol 5:486–488
7. Vassar R, Bennett BD, Babu-Khan S, Kahn S, Mendiaz EA, Denis P, Teplow DB, Ross S, Amarante P, Loeloff R et al (1999) beta-Secretase cleavage of Alzheimer's amyloid precursor protein by the transmembrane aspartic protease BACE. Science 286:735–741
8. Steiner H (2004) Uncovering gamma-secretase. Curr Alzheimer Res 1:175–181
9. Saunders AM, Strittmatter WJ, Schmechel D, George-Hyslop PH, Pericak-Vance MA, Joo SH, Rosi BL, Gusella JF, Crapper-MacLachlan DR, Alberts MJ et al (1993) Association of apolipoprotein E allele epsilon 4 with late-onset familial and sporadic Alzheimer's disease. Neurology 43:1467–1472
10. Bu G (2009) Apolipoprotein E and its receptors in Alzheimer's disease: pathways, pathogenesis and therapy. Nat Rev Neurosci 10:333–344
11. Kovacs DM (2000) alpha2-Macroglobulin in late-onset Alzheimer's disease. Exp Gerontol 35:473–479
12. Dodson SE, Andersen OM, Karmali V, Fritz JJ, Cheng D, Peng J, Levey AI, Willnow TE, Lah JJ (2008) Loss of LR11/SORLA enhances early pathology in a mouse model of amyloidosis: evidence for a proximal role in Alzheimer's disease. J Neurosci 28:12877–12886
13. Rogaeva E, Meng Y, Lee JH, Gu Y, Kawarai T, Zou F, Katayama T, Baldwin CT, Cheng R, Hasegawa H et al (2007) The neuronal sortilin-related receptor SORL1 is genetically associated with Alzheimer disease. Nat Genet 39:168–177
14. Zhao Z, Ho L, Wang J, Qin W, Festa ED, Mobbs C, Hof P, Rocher A, Masur S, Haroutunian V, Pasinetti GM (2005) Connective tissue growth factor (CTGF) expression in the brain is a downstream effector of insulin resistance- associated promotion of Alzheimer's disease beta-amyloid neuropathology. FASEB J 19:2081–2082
15. Kang DE, Pietrzik CU, Baum L, Chevallier N, Merriam DE, Kounnas MZ, Wagner SL, Troncoso JC, Kawas CH, Katzman R, Koo EH (2000) Modulation of amyloid beta-protein clearance and Alzheimer's disease susceptibility by the LDL receptor-related protein pathway. J Clin Invest 106:1159–1166
16. Segarini PR, Nesbitt JE, Li D, Hays LG, Yates JR 3rd, Carmichael DF (2001) The low density lipoprotein receptor-related protein/alpha2-macroglobulin receptor is a receptor for connective tissue growth factor. J Biol Chem 276:40659–40667
17. Spoelgen R, Adams KW, Koker M, Thomas AV, Andersen OM, Hallett PJ, Bercury KK, Joyner DF, Deng M, Stoothoff WH et al (2009) Interaction of the apolipoprotein E receptors low density lipoprotein receptor-related protein and sorLA/LR11. Neuroscience 158:1460–1468
18. Keene CD, Rodrigues CM, Eich T, Chhabra MS, Steer CJ, Low WC (2002) Tauroursodeoxycholic acid, a bile acid, is neuroprotective in a transgenic animal model of Huntington's disease. Proc Natl Acad Sci U S A 99:10671–10676
19. Keene CD, Rodrigues CM, Eich T, Linehan-Stieers C, Abt A, Kren BT, Steer CJ, Low WC (2001) A bile acid protects against motor and cognitive deficits and reduces striatal degeneration in the 3-nitropropionic acid model of Huntington's disease. Exp Neurol 171:351–360
20. Rodrigues CM, Sola S, Nan Z, Castro RE, Ribeiro PS, Low WC, Steer CJ (2003) Tauroursodeoxycholic acid reduces apoptosis and protects against neurological injury after acute hemorrhagic stroke in rats. Proc Natl Acad Sci U S A 100:6087–6092
21. Rodrigues CM, Spellman SR, Sola S, Grande AW, Linehan-Stieers C, Low WC, Steer CJ (2002) Neuroprotection by a bile acid in an acute stroke model in the rat. J Cereb Blood Flow Metab 22:463–471
22. Viana RJ, Ramalho RM, Nunes AF, Steer CJ, Rodrigues CM (2010) Modulation of amyloid-beta peptide-induced toxicity through inhibition of JNK nuclear localization and caspase-2 activation. J Alzheimers Dis 22:557–568
23. Ramalho RM, Borralho PM, Castro RE, Sola S, Steer CJ, Rodrigues CM (2006) Tauroursodeoxycholic acid modulates p53-mediated apoptosis in Alzheimer's disease mutant neuroblastoma cells. J Neurochem 98:1610–1618
24. Ramalho RM, Ribeiro PS, Sola S, Castro RE, Steer CJ, Rodrigues CM (2004) Inhibition of the E2F-1/p53/Bax pathway by tauroursodeoxycholic acid in amyloid beta-peptide-induced apoptosis of PC12 cells. J Neurochem 90:567–575
25. Sola S, Amaral JD, Borralho PM, Ramalho RM, Castro RE, Aranha MM, Steer CJ, Rodrigues CM (2006) Functional modulation of nuclear steroid receptors by tauroursodeoxycholic acid reduces amyloid beta-peptide-induced apoptosis. Mol Endocrinol 20:2292–2303
26. Viana RJ, Nunes AF, Castro RE, Ramalho RM, Meyerson J, Fossati S, Ghiso J, Rostagno A, Rodrigues CM (2009) Tauroursodeoxycholic

acid prevents E22Q Alzheimer's Abeta toxicity in human cerebral endothelial cells. Cell Mol Life Sci 66:1094–1104
27. Castro RE, Sola S, Ma X, Ramalho RM, Kren BT, Steer CJ, Rodrigues CM (2005) A distinct microarray gene expression profile in primary rat hepatocytes incubated with ursodeoxycholic acid. J Hepatol 42:897–906
28. Parry GJ, Rodrigues CM, Aranha MM, Hilbert SJ, Davey C, Kelkar P, Low WC, Steer CJ (2010) Safety, tolerability, and cerebrospinal fluid penetration of ursodeoxycholic acid in patients with amyotrophic lateral sclerosis. Clin Neuropharmacol 33:17–21
29. Radde R, Bolmont T, Kaeser SA, Coomaraswamy J, Lindau D, Stoltze L, Calhoun ME, Jaggi F, Wolburg H, Gengler S et al (2006) Abeta42-driven cerebral amyloidosis in transgenic mice reveals early and robust pathology. EMBO Rep 7:940–946
30. Crosignani A, Setchell KD, Invernizzi P, Larghi A, Rodrigues CM, Podda M (1996) Clinical pharmacokinetics of therapeutic bile acids. Clin Pharmacokinet 30:333–358
31. Castro RE, Ferreira DM, Zhang X, Borralho PM, Sarver AL, Zeng Y, Steer CJ, Kren BT, Rodrigues CM (2010) Identification of microRNAs during rat liver regeneration after partial hepatectomy and modulation by ursodeoxycholic acid. Am J Physiol Gastrointest Liver Physiol 299:G887–G897
32. Goddyn H, Callaerts-Vegh Z, Stroobants S, Dirikx T, Vansteenwegen D, Hermans D, van der Putten H, D'Hooge R (2008) Deficits in acquisition and extinction of conditioned responses in mGluR7 knockout mice. Neurobiol Learn Mem 90:103–111
33. Yu Z, Xu X, Xiang Z, Zhou J, Zhang Z, Hu C, He C (2010) Nitrated alpha-synuclein induces the loss of dopaminergic neurons in the substantia nigra of rats. PLoS One 5:e9956
34. Sola S, Xavier JM, Santos DM, Aranha MM, Morgado AL, Jepsen K, Rodrigues CM (2011) p53 interaction with JMJD3 results in its nuclear distribution during mouse neural stem cell differentiation. PLoS One 6:e18421
35. Borralho PM, Simoes AE, Gomes SE, Lima RT, Carvalho T, Ferreira DM, Vasconcelos MH, Castro RE, Rodrigues CM (2011) miR-143 overexpression impairs growth of human colon carcinoma xenografts in mice with induction of apoptosis and inhibition of proliferation. PLoS One 6:e23787
36. Blanchard V, Moussaoui S, Czech C, Touchet N, Bonici B, Planche M, Canton T, Jedidi I, Gohin M, Wirths O et al (2003) Time sequence of maturation of dystrophic neurites associated with Abeta deposits in APP/PS1 transgenic mice. Exp Neurol 184:247–263
37. Jankowsky JL, Fadale DJ, Anderson J, Xu GM, Gonzales V, Jenkins NA, Copeland NG, Lee MK, Younkin LH, Wagner SL et al (2004) Mutant presenilins specifically elevate the levels of the 42 residue beta-amyloid peptide in vivo: evidence for augmentation of a 42-specific gamma secretase. Hum Mol Genet 13:159–170
38. Trinchese F, Liu S, Battaglia F, Walter S, Mathews PM, Arancio O (2004) Progressive age-related development of Alzheimer-like pathology in APP/PS1 mice. Ann Neurol 55:801–814
39. Itagaki S, McGeer PL, Akiyama H, Zhu S, Selkoe D (1989) Relationship of microglia and astrocytes to amyloid deposits of Alzheimer disease. J Neuroimmunol 24:173–182
40. Matsuoka Y, Picciano M, Malester B, LaFrancois J, Zehr C, Daeschner JM, Olschowka JA, Fonseca MI, O'Banion MK, Tenner AJ et al (2001) Inflammatory responses to amyloidosis in a transgenic mouse model of Alzheimer's disease. Am J Pathol 158:1345–1354
41. McGeer EG, McGeer PL (1999) Brain inflammation in Alzheimer disease and the therapeutic implications. Curr Pharm Des 5:821–836
42. West MJ, Coleman PD, Flood DG, Troncoso JC (1994) Differences in the pattern of hippocampal neuronal loss in normal ageing and Alzheimer's disease. Lancet 344:769–772
43. Fonseca MI, Zhou J, Botto M, Tenner AJ (2004) Absence of C1q leads to less neuropathology in transgenic mouse models of Alzheimer's disease. J Neurosci 24:6457–6465
44. Rupp NJ, Wegenast-Braun BM, Radde R, Calhoun ME, Jucker M (2011) Early onset amyloid lesions lead to severe neuritic abnormalities and local, but not global neuron loss in APPPS1 transgenic mice. Neurobiol Aging 32(2324):e2321–e2326
45. Borchelt DR, Thinakaran G, Eckman CB, Lee MK, Davenport F, Ratovitsky T, Prada CM, Kim G, Seekins S, Yager D et al (1996) Familial Alzheimer's disease-linked presenilin 1 variants elevate Abeta1-42/1-40 ratio in vitro and in vivo. Neuron 17:1005–1013
46. Selkoe D, Kopan R (2003) Notch and Presenilin: regulated intramembrane proteolysis links development and degeneration. Annu Rev Neurosci 26:565–597
47. Evin G, Sernee MF, Masters CL (2006) Inhibition of gamma-secretase as a therapeutic intervention for Alzheimer's disease: prospects, limitations and strategies. CNS Drugs 20:351–372
48. Scherzer CR, Offe K, Gearing M, Rees HD, Fang G, Heilman CJ, Schaller C, Bujo H, Levey AI, Lah JJ (2004) Loss of apolipoprotein E receptor LR11 in Alzheimer disease. Arch Neurol 61:1200–1205
49. Ohki Y, Higo T, Uemura K, Shimada N, Osawa S, Berezovska O, Yokoshima S, Fukuyama T, Tomita T, Iwatsubo T (2011) Phenylpiperidine-type gamma-secretase modulators target the transmembrane domain 1 of presenilin 1. EMBO J 30:4815–4824
50. Burns MP, Noble WJ, Olm V, Gaynor K, Casey E, LaFrancois J, Wang L, Duff K (2003) Co-localization of cholesterol, apolipoprotein E and fibrillar Abeta in amyloid plaques. Brain Res Mol Brain Res 110:119–125
51. Van Gool D, De Strooper B, Van Leuven F, Triau E, Dom R (1993) alpha 2-Macroglobulin expression in neuritic-type plaques in patients with Alzheimer's disease. Neurobiol Aging 14:233–237
52. Ben Mosbah I, Alfany-Fernandez I, Martel C, Zaouali MA, Bintanel-Morcillo M, Rimola A, Rodes J, Brenner C, Rosello-Catafau J, Peralta C (2010) Endoplasmic reticulum stress inhibition protects steatotic and non-steatotic livers in partial hepatectomy under ischemia–reperfusion. Cell Death Dis 1:e52
53. Seyhun E, Malo A, Schafer C, Moskaluk CA, Hoffmann RT, Goke B, Kubisch CH (2011) Tauroursodeoxycholic acid reduces endoplasmic reticulum stress, acinar cell damage, and systemic inflammation in acute pancreatitis. Am J Physiol Gastrointest Liver Physiol 301:G773–G782
54. Calhoun ME, Wiederhold KH, Abramowski D, Phinney AL, Probst A, Sturchler-Pierrat C, Staufenbiel M, Sommer B, Jucker M (1998) Neuron loss in APP transgenic mice. Nature 395:755–756